Journal of Biomedical Research

Hypoxia-induced acidic microenvironment alters cellular pharmacokinetics of gastric cancer in a Mongolian population

Jiawen Cheng, Zhouyue Wu, Mengran Wang, Liguo Wang, Chenchen Jiang, Xiang Chen, Minghui Zhang, Le Xia, Tingting Yang, Lulu Zhang, Xuezhi Wang, Yixuan Zhang

Cite this article as:
Jiawen Cheng, Zhouyue Wu, Mengran Wang, Liguo Wang, Chenchen Jiang, Xiang Chen, Minghui Zhang, Le Xia, Tingting Yang, Lulu Zhang, Xuezhi Wang, Yixuan Zhang. Hypoxia-induced acidic microenvironment alters cellular pharmacokinetics of gastric cancer in a Mongolian population[J]. *Journal of Biomedical Research*, In press. doi: 10.7555/JBR.39.20250238

View online: https://doi.org/10.7555/JBR.39.20250238

Available online at www.jbr-pub.org.cn

Open Access at PubMed Central

Journal of Biomedical Research, 2026 40(0): 1–18

JBR

Original Article

Hypoxia-induced acidic microenvironment alters cellular pharmacokinetics of gastric cancer in a Mongolian population

Jiawen Cheng[1,△], Zhouyue Wu[2,△], Mengran Wang[3,4,△], Liguo Wang[3,4], Chenchen Jiang[2], Xiang Chen[2], Minghui Zhang[4], Le Xia[2,6], Tingting Yang[2,6], Lulu Zhang[2], Xuezhi Wang[3,4,✉], Yixuan Zhang[2,5,✉]

[1]*Department of Physiology, School of Basic Medical Sciences, Nanjing Medical University, Nanjing, 211166, China;*
[2]*Medical Basic Research Innovation Center for Cardiovascular and Cerebrovascular Diseases, Ministry of Education, China; International Joint Laboratory for Drug Target of Critical Illnesses, School of Pharmacy, Nanjing Medical University, Nanjing 211166, China;*
[3]*Affiliated Chifeng Clinical College of Inner Mongolia Medical University, Chifeng 024000, China;*
[4]*Department of Tumor Surgery, Chifeng Municipal Hospital, Chifeng 024000, China;*
[5]*The affiliated Huaian No.1 People's Hospital of Nanjing Medical University, Northern Jiangsu Institute of Clinical Medicine, Huaian 223300, China;*
[6]*School of Tianyuan Honors, Nanjing Medical University, Nanjing, 211166, China.*

Abstract

This study aims to comprehensively analyze the transcriptome characteristics of Mongolian gastric cancer (GC) patients to elucidate the critical molecular events underlying treatment response in this ethnic population. The objective is to establish connections between these molecular events and the cellular pharmacokinetics of chemotherapy drugs. Our investigation revealed increased activation of the hypoxia pathway in GC tumor tissues from Mongolian individuals, which was significantly associated with adverse prognosis. Through analysis of hypoxia-induced changes in cellular pharmacokinetics, we identified three chemotherapy drugs —paclitaxel, oxaliplatin, and tegafur–gimeracil–oteracil potassium capsules (TGO) —that exhibit distinct transport and metabolic characteristics in GC tumor cells of Mongolian nationality. These findings provide valuable insights for clinical practice, particularly in refining treatment strategies and advancing personalized medicine for Mongolian GC patients.

Keywords: Cellular Pharmacokinetics, Mongolian population, Gastric Cancer, Tumor microenvironment

Introduction

Among existing chemotherapy drugs available on the market, including both targeted and cytotoxic agents, most explicitly state in their Food and Drug Administration (FDA) submission materials that they have not undergone in-depth research regarding ethnic disparities. However, real-world empirical studies suggest that variations in therapeutic outcomes persist for certain cancer drugs across diverse ethnic groups, potentially exerting a substantial impact on long-term patient prognosis[1, 2]. Thoroughly identifying genetic and transcriptional variations and investigating their contributions to health and disease, in conjunction

△These authors contributed equally to this work.

✉Corresponding authors: Xuezhi Wang, E-mail: wangxuezhi0117@126.com; Yi-Xuan Zhang, E-mail: yxzhang@njmu.edu.cn.

Received: 07 June 2025; Revised: 24 March 2026; Accepted: 27 March 2026;

CLC number: R735.2; R969.1, Document code: A

The authors reported no conflict of interests.

https://doi.org/10.7555/JBR.39.20250238

with environmental and lifestyle factors, will enhance the precision of cancer treatment[3]. A significant challenge in advancing this research is the historical underrepresentation of diverse populations in biomedical studies, including those from varied ancestries, geographical environments, and lifestyles[4]. For instance, Mongolian and Han ethnic groups exhibit distinct genetic and transcriptional backgrounds[5], as well as different lifestyles. Yet, existing gastric cancer treatment guidelines fail to account for these variations[6, 7], resulting in a lack of precise treatment options for Mongolian patients.

Mongolians traditionally maintain a lifestyle centered around animal husbandry, which differs markedly from the dietary habits of the Han Chinese. Multiple epidemiological studies have revealed a strong association between gastric cancer (GC) and *Helicobacter pylori* (*H. pylori*) infection, with previous research indicating a significant incidence of *H. pylori* infection among Mongolians[8]. These divergences in lifestyle and diet may influence the mechanisms underlying GC development. Past research has predominantly focused on the epidemiological characteristics of GC in the Han population[9], with comparatively limited in-depth examination of GC in Mongolians. Consequently, we posit that a thorough exploration of tumor heterogeneity between Mongolian and Han populations will provide crucial insights for tailoring prevention and treatment strategies specific to Mongolian GC patients.

This study aims to analyze the cellular pharmacokinetics of chemotherapy drugs commonly used in Mongolian GC patients using transcriptomic data, with the goal of uncovering the molecular mechanisms driving cellular pharmacokinetics and exploring their therapeutic implications. Our findings reveal significant activation of the hypoxia pathway in tumor tissues from Mongolian GC patients, offering new insights into disease progression. By leveraging the impact of hypoxia on drug metabolism in tumor cells, we identified three chemotherapy agents that may be particularly suitable for this population. This optimization is grounded in a comprehensive understanding of how hypoxia pathways influence cellular pharmacokinetics. Overall, this research deepens our insights into the molecular mechanism underlying GC development in Mongolians through transcriptomic analysis, laying a robust foundation for implementing more precise personalized treatment strategies. These results underscore the pivotal role of cellular pharmacokinetics research in elucidating tumor pathological mechanisms and guiding individualized therapy, offering new directions for future innovation in GC treatment.

Materials and methods

Study approval

All samples were obtained from the GC biobank at Chifeng Municipal Hospital in the Inner Mongolia Autonomous Region. Sample collection, storage, and analysis, along with the handling of clinical data, adhered to the standards of the Declaration of Helsinki and were approved by the Ethics Committee of Chifeng Municipal Hospital (Approval No. 2017-40). The study was conducted with the understanding and written informed consent of each participant. Clinical information of the samples is provided in ***Supplementary Table 1***.

Immunohistochemistry (IHC) analysis

IHC was performed on 3-μm-thick sections of paraffin-embedded GC tumor tissues and paired adjacent non-tumor tissues. Sections were deparaffinized, rehydrated, and subjected to antigen retrieval in citrate buffer (pH 6.0), followed by incubation with 3% hydrogen peroxide and blocking with 3% goat serum. Subsequently, sections were incubated overnight at 4 ℃ with a primary antibody against CA12 (1 : 500; Cat. #15180-1-AP, Proteintech, Rosemont, USA). After washing with phosphate buffered saline sections were incubated with a horseradish peroxidase (HRP)-conjugated secondary antibody for 50 min at room temperature. Immunoreactive signals were visualized using 3,3'-diaminobenzidine (DAB) substrate, and nuclei were counterstained with hematoxylin.

Western blotting analysis

Cells were harvested and lysed in cell lysis buffer supplemented with protease inhibitors, followed by incubation on ice for 30 min. Lysates were centrifuged at 12 500 *g* for 30 min at 4 ℃, and the supernatants were collected. Protein concentrations were determined using the Pierce BCA Protein Assay Kit (Thermo Fisher Scientific, MA, USA). Equal amounts of protein were denatured in SDS-Laemmli buffer at 95 ℃ for 5 min, separated by Bis-Tris SDS-PAGE gels, and transferred onto PVDF membranes. Membranes were blocked with 5% non-fat dry milk in TBS-T for 1 h at room temperature and then incubated at 4 ℃ overnight with primary antibodies against CA12 (1 : 5 000; Cat. #15180-1-AP, Proteintech) and β-actin (1 : 5 000; Cat. #66009-1-Ig, Proteintech). After washing,

membranes were incubated with the corresponding HRP-conjugated secondary antibodies (1∶5 000, Cat. #SA00001-2, Proteintech; and 1∶5 000, Cat. #SA00001-1, Proteintech) at room temperature for 2 h. Immunoreactive signals were detected using enhanced chemiluminescence (ECL) reagents, and images were captured using the Tanon Digital Gel Imaging System (Tanon Life Science Co., Ltd., Shanghai, China).

Real-time quantitative PCR (RT-qPCR) analysis

Total RNA was extracted using RNAiso Plus (Cat. #9109, Takara, Kusatsu, Japan) and reverse-transcribed into cDNA using the HiScript II Q RT SuperMix for qPCR kit (Cat. #R223-01, Vazyme, Nanjing, China) according to the manufacturer's instructions. RT-qPCR was performed in Hard-Shell 384-well PCR plates (Cat. #HSP3801, Bio-Rad, Hercules, USA) on a Real-Time PCR system (Applied Biosystems, Waltham, USA) using the AceQ qPCR SYBR Green Master Mix (Cat. #Q131-02, Vazyme). The primer sequences used were as follows:

CYP3A4 (forward, 5′-GTGTGGGGCTTTTATGATGGTC-3′; reverse, 5′-GACCAAAAGGCCTCCGGTTT-3′), *SLCO1B3* (forward, 5′-ACCAAGGCATCGGACAATGAA-3′; reverse, 5′-CAGCAGCATTGTCTTGCATGT-3′), *SLC22A2* (forward, 5′-GGCTTACGCACTTCCTCACT-3′; reverse, 5′-AGGGAGGCGGGTAGAGATTT-3′), *CYP2C8* (forward, 5′-TCTTTCACCAATTTCTCAAAAGTCT-3′; reverse, 5′-TGGAAATGATTCCAAGTCCTTTAGT-3′), *SLC22A3* (forward, 5′-GAGGAGTGGAACCGCACG-3′; reverse, 5′-CACAGACAAGGTCAAACTCGC-3′), *CYP2E1* (forward, 5′-TGCAACGTCATAGCCGACAT-3′; reverse, 5′-TGGCTTCCAGGCAAGTAGTG-3′), and *ACTB* (forward, 5′-AGGGCTGCTTTTAACTCTGGT-3′; reverse, 5′-CCCCACTTGATTTTGGAGGGA-3′). Relative mRNA expression levels were normalized to *ACTB* and calculated using the $2^{-\Delta\Delta Ct}$ method[10].

Cell culture

The SGC-7901 human gastric cancer cell line was kindly provided by Prof. Xiying Tan (The First Clinical Medical College, Nanjing University of Chinese Medicine). Cells were cultured in RPMI-1640 medium (Gibco, CA, USA) supplemented with 10% fetal bovine serum (Gibco). Cultures were maintained at 37 ℃ in a humidified incubator with 5% CO_2.

For hypoxia experiments, cells were placed in a hypoxia chamber (1% O_2) and purged with a gas mixture of 95% N_2 and 5% CO_2 for 15 min until the oxygen concentration stabilized below 1%, followed by incubation under hypoxic conditions for 36 h. Normoxic control cells were cultured under identical conditions in a standard atmosphere (21% O_2 and 5% CO_2).

Tumor cell-based drug-sensitivity assay

Cell viability was assessed using the Cell Counting Kit-8 (CCK-8; Cat. #K1018; APExBIO, Houston, USA). SGC-7901 cells were seeded in 96-well plates at a density of 7 000 cells per well and allowed to adhere overnight. Subsequently, cells were treated with varying concentrations of paclitaxel (Cat. #HY-B0015, MedChemExpress, New Jersey, USA) or oxaliplatin (Cat. #HY-17371, MedChemExpress) for 36 h. Following treatment, the culture medium was replaced with 100 μL of CCK-8 working solution (prepared by diluting the stock solution 1∶10 in culture medium). Plates were incubated at 37 ℃ for 2 h. The optical detection wavelength was 450 nm.

RNA sequencing and data analysis

Total RNA was extracted using TRIzol reagent (Invitrogen, CA, USA) according to the manufacturer's protocol. RNA quality and quantity were assessed using an Agilent 2 100 Bioanalyzer (Agilent Technologies, Santa Clara, CA, USA), and a NanoDrop 2 000 spectrophotometer (Thermo Fisher Scientific). Libraries were constructed and sequenced on an Illumina Novaseq 6 000 platform to generate 150-bp paired-end reads. Reference transcriptome sequencing was performed on all 17 samples, including four Mongolian GC tumors, five Mongolian GC adjacent non-tumor tissues, three Han GC tumors, and five Han GC adjacent non-tumor tissues. A total of 114.30 Gb of clean data was obtained by removing sequences with base quality scores lower than 20. The effective data volume per sample ranged from 6.48 to 7.02 Gb, with Q30 scores between 93.08% and 93.91% and an average GC content of 51.37%. By comparing reads to the Human genome using HISAT, the genome alignment of each sample was obtained, with an alignment rate of 95.10% to 97.14%. Gene expression levels were quantified as fragments per kilobase of transcript per million mapped reads (FPKM), and raw read counts were generated using HTSeq-count.

Data acquisition from The Cancer Genome Atlas (TCGA)-Stomach Adenocarcinoma (STAD)

Transcriptomic and clinical data for the TCGA-STAD cohort were downloaded from the UCSC Xena browser (https://xena.ucsc.edu/).

Principal component analysis (PCA)

PCA, a widely adopted linear dimensionality reduction technique, was employed for data preprocessing[11]. This method quantifies data variability through variance measurement and projects high-dimensional data featuring significant differences onto a lower-dimensional space. PCA was performed using the R package FactoMineR (version 2.8), which automatically standardizes data prior to analysis. After PCA, two principal components, Principal Component 1 (PC1) and PC2, were derived to represent the directions with the highest and second-highest data variability, respectively. Group disparities were visualized using the ggplot2 package (version 3.4.2)[12].

Differentially expressed gene (DEG) analysis

DEG analysis was performed using the R package DESeq2 (version 1.38.3)[13]. This method quantifies alterations in gene expression between two groups by calculating the fold change. DEGs were identified using the thresholds of a *P-value* < 0.05 and $|\log_2(\text{fold change})| > 1$. The results were visualized as a volcano plot generated using the R package EnhancedVolcano (version 1.16.0).

Gene Ontology (GO) enrichment analysis

GO enrichment analysis was performed to identify whether differentially expressed genes were significantly enriched in specific molecular functions, biological processes, or cellular components as defined in the GO database[14]. The functional enrichment analysis was conducted using the R package clusterProfiler (version 4.7.1.3)[15] with a significance threshold set at a *P-value* < 0.05 and a *q-value* < 0.2. Results visualization was conducted using bar plots and bubble charts created with the R package ggplot2 (version 3.4.2)[12].

Kyoto Encyclopedia of Genes and Genomes (KEGG) enrichment analysis

KEGG enrichment analysis was performed to identify biological pathways significantly enriched among DEGs[16]. Functional enrichment analysis was conducted using the R package clusterProfiler (version 4.7.1.3)[15], with a significance threshold set at a *P-value* < 0.05 and a *q-value* < 0.2. Results were visualized as bar plots and bubble charts using the R package ggplot2 (version 3.4.2)[12].

Pathway activity analysis

Pathway activity was inferred using the R package PROGENy (version 1.17.3), which estimates pathway activity based on the expression of pathway-responsive genes rather than the full pathway gene set[17]. RNA-seq data were preprocessed and normalized to FPKM values before analysis. Pathway scores were calculated using the top 100 responsive genes per pathway and subsequently z-score-normalized across samples to yield unitless values reflecting relative pathway activity. In total, 14 pathway activities were inferred using default parameters.

Gene Set Enrichment Analysis (GSEA)

GSEA was performed using GSEA software (version 4.2.3) to identify predefined gene sets showing statistically significant and concordant differences between two biological states. A significance threshold of a *P-value* < 0.05 and false discovery rate (FDR, Benjamini–Hochberg–adjusted) < 0.25 was applied for statistical significance[18]. Results were visualized using the R package GseaVis (version 0.0.8).

Correlation analysis

The R package corrplot (version 0.92) was used to analyze and visualize the correlation matrix. Correlation analysis was employed to investigate associations among the Genecards GC-Mongolian Hypoxia (GGC-MH) gene set. Specifically, the Pearson correlation coefficient was used, and statistical significance was assessed by calculating *P-values* using the 'cor.mtest' function. A threshold of $P < 0.05$ was applied to define significant correlations.

Survival analysis

Kaplan-Meier survival curves were generated to evaluate the association between gene expression levels and patient survival outcomes. We employed the R package survival (version 3.5.5) to calculate Kaplan-Meier survival estimates and used survminer (version 0.4.9) for summarizing and visualizing the survival analysis results. In survival analysis, the log-rank test was applied to obtain *P-values*, determining whether there is a significant difference in survival distributions between two groups.

Construction of Protein-Protein Interaction (PPI) network

PPI networks were constructed to explore physical interactions among proteins, which are crucial for deciphering various cellular processes, signaling pathways, and potential disease mechanisms. The Search Tool for the Retrieval of Interacting

Genes/Proteins (STRING) is an online database and tool designed for studying PPI (https://string-db.org/). The STRING database compiles extensive information on protein interactions, encompassing both known and predicted interactions. The resulting interaction networks were imported into the Cytoscape software (version 3.10.3) for visualization.

Drug sensitivity analysis

The R package oncoPredict (version 0.2)[19], a computational tool designed for drug sensitivity analysis, was employed to evaluate the response of GC tumor tissues to various chemotherapy drugs. Drug response models were trained on the Genomics of Drug Sensitivity in Cancer, version 2 (GDSC2) reference dataset, which includes RMA-normalized, log-transformed gene expression profiles and corresponding half maximal inhibitory concentration (IC_{50}) values. Ridge regression, as implemented in oncoPredict, was used to fit the drug response models.

Clinical cohort study

A clinical cohort study was conducted involving GC inpatients treated at the Department of Tumor Surgery of Chifeng Municipal Hospital, between January 2019 and December 2024. Data collection adhered to the principles of the Declaration of Helsinki and was approved by the Ethics Committee of Chifeng Municipal Hospital (Approval No. CK2021014). Patients were screened according to predefined inclusion and exclusion criteria.

Data and statistical analyses

All experimental data were presented as the mean ± standard error of the mean (SEM) using Prism v.8.0.1 (GraphPad Software). For direct comparisons between two groups, a two-tailed unpaired Student's *t*-test was used. For comparisons among multiple groups, one-way or two-way analysis of variance (ANOVA) was performed, followed by Tukey's or Bonferroni's post-hoc test for multiple comparisons. A *P*-value < 0.05 was considered statistically significant.

Results

Hypoxia pathway is specifically activated in GC tissues of Mongolian patients

Our study involved paired-end transcriptome sequencing for each sample, resulting in quantified expression data for 16 615 protein-coding genes following quality control and preprocessing. PCA initially demonstrated a clear separation between Mongolian GC tumor tissues and adjacent non-tumor tissues (***Fig. 1A***). Differential expression analysis using DESeq2 revealed 1 214 downregulated genes and 1 610 upregulated genes in tumor tissues compared with controls. Among these, *KRT6B* exhibited the most significant alteration (***Fig. 1B*** and ***Supplementary Table 2***). While previous studies have linked elevated *KRT6B* expression to the occurrence and progression of certain cancers[20, 21], its role in GC remains less characterized, warranting further investigation. Additionally, genes extensively reported to be upregulated in GC, such as *ERBB2*, *BRCA1*, and *FAT1*[22, 23], were also upregulated in Mongolian GC patients (***Fig. 1C***). Further investigation through GO and KEGG functional enrichment analyses unveiled significant changes in terms related to the regulation of endocrine processes, gastric acid secretion, the IL-17 signaling pathway, proteoglycans in cancer, among others, all of which align with established GC pathological mechanisms[24, 25] (***Supplementary Fig. 1A***).

Aberrant signaling pathways play a pivotal role in cancer progression. To elucidate the molecular alterations specific to Mongolian GC, we employed PROGENy to infer pathway activities based on gene expression profiles. This approach provided a nuanced understanding of the molecular landscape characterizing GC in this population. Our findings revealed significant activation of the mitogen-activated protein kinase (MAPK), hypoxia, epidermal growth factor receptor (EGFR), nuclear factor kappa-B (NF-κB), and TNF-related apoptosis-inducing ligand (TRAIL) pathways in Mongolian GC patients (***Fig. 1D***). Further analysis of TCGA-STAD[26] highlighted a specific activation of the hypoxia pathway in Mongolian patients compared with other ethnic groups (***Fig. 1E*** and ***Supplementary Fig. 1B*** and ***1C***). This observation was further corroborated by GSEA (***Supplementary Fig. 1D***).

PROGENy provides a comprehensive method for assessing pathway activity. To further elucidate the relationship between gene expression and cellular signaling, we curated a hypoxia-related gene set from the Molecular Signatures Database (MSigDB), identifying a total of 317 genes (***Supplementary Table 3***). Among these genes, 14 were upregulated and 35 were downregulated (***Fig. 1F***). To validate our transcriptomic findings, we focused on *CA12*, a hypoxia-inducible transmembrane carbonic anhydrase that catalyzes the hydration of CO_2 to maintain intracellular pH[27], thereby sustaining tumor-cell survival under hypoxic stress and intensifying intratumoral hypoxia to drive a more aggressive

phenotype[28]. IHC analysis of Mongolian GC tumor tissues confirmed markedly elevated CA12 protein levels (Fig. 1G). Consistently, Western blot analysis in SGC-7 901 cells showed that 36 hours of hypoxia

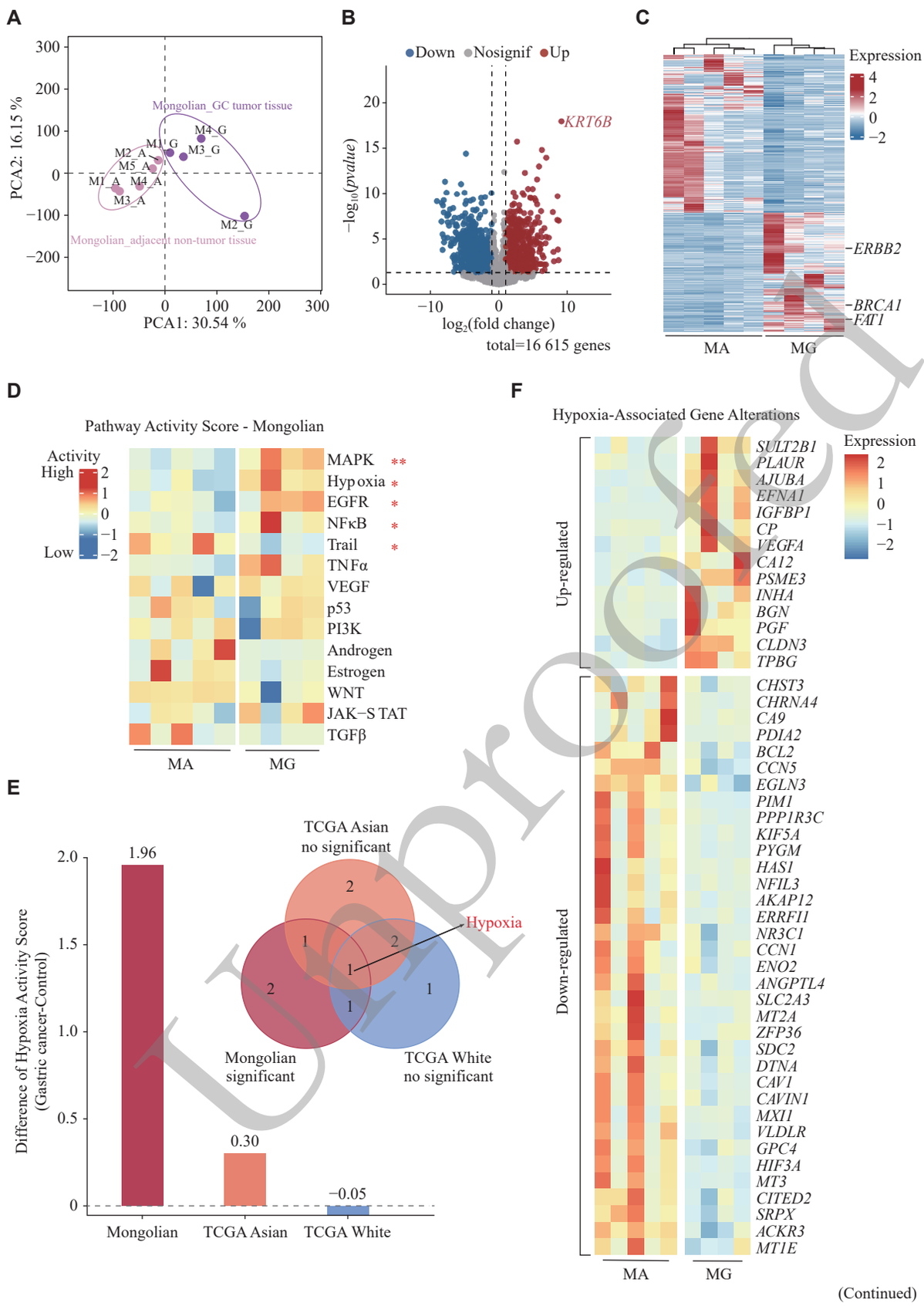

(Continued)

(Continued)

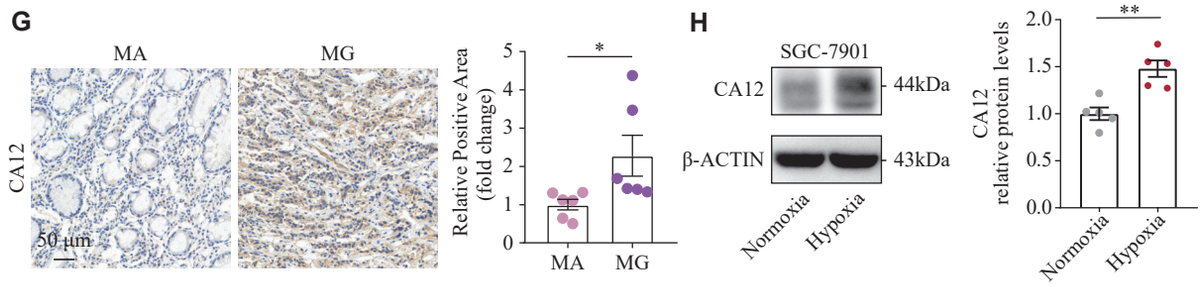

Fig. 1 **Differential gene expression (DEG) and cancer-related pathway analysis in Mongolian gastric cancer (GC) and adjacent non-tumor tissues.** A: PCA illustrates the distribution of samples along principal components (Mongolian GC tumor tissues *vs*. adjacent non-tumor tissues). Each point represents an individual sample (Mongolian adjacent non-tumor tissues, $n = 5$; Mongolian GC tumor tissues, $n = 4$). B: Volcano plot visualizing DEGs identified by the Wald test in DESeq2. Red dots represent upregulated genes ($P < 0.05$; fold change > 2), blue dots represent downregulated genes ($P < 0.05$, fold change < −2), and gray dots represent genes with no significant differential expression. C: Heatmap illustrating DEGs in Mongolian GC tumor tissues ($n = 4$) compared with adjacent non-tumor tissues ($n = 5$). D: Heatmap illustrating pathway activity scores in Mongolian GC tumor tissues ($n = 4$) compared with adjacent non-tumor tissues ($n = 5$). $^{*}P < 0.05$, $^{**}P < 0.01$ by two-tailed Student's *t* test. E: Top right: Venn diagram depicting the specific and shared activated pathway counts in Mongolian GC tumor tissues relative to TCGA Asian and TCGA White (compared with adjacent non-tumor tissues). Bottom left: Bar chart illustrating the differences of hypoxia activity scores for Mongolian, TCGA Asian, and TCGA White, with differences retained to two decimal places. F: Heatmap illustrating hypoxia-associated genes in Mongolian GC tumor tissues ($n = 4$) compared with adjacent non-tumor tissues ($n = 5$). G: Left: Representative immunohistochemical staining of CA12 in Mongolian GC tissue and adjacent non-tumor. Scale bar = 50 μm. Right: Quantification of CA12-positive area relative to total tissue area was performed using ImageJ. Data are presented as mean ± standard error of the mean (SEM). $^{*}P < 0.05$ by two-tailed Student's *t* test ($n = 6$). H: Representative bands and quantification of the protein level of CA12 in SGC-7 901 cells after 36 hours of hypoxia exposure. Data are presented as mean ± SEM ($n = 5$; $^{**}P < 0.01$), two-tailed Student's *t* test. Abbreviations: MG, Mongolian GC tumor tissue; MA, Mongolian adjacent non-tumor tissue; PCA, principal component analysis; TCGA, The Cancer Genome Atlas.

exposure induced a marked increase in CA12 protein expression (**Fig. 1H**), further supporting hypoxia-driven CA12 activation at the cellular level. We hypothesize that these genes play crucial roles in the pathogenesis of GC in the Mongolian population.

Association between hypoxia and poor prognosis in Mongolian GC patients

To substantiate the association between hypoxia and GC, we systematically queried the GeneCards database for GC-associated protein-coding genes, yielding a total of 9 576 candidates. We then ranked the top 100%, 75%, 50%, and 25% of genes based on theRelevanceScoreindescendingorderandselected4 788 genes using the median Relevance Score as a criterion. Intersection analysis between these 4 788 GeneCards-derived genes and the hypoxia-related DEGs identified in Mongolian GC patients revealed a substantial overlap: 37 out of the 49 Mongolian hypoxia-related genes were present in the GeneCards GC-related gene set (***Fig. 2A*** and ***Supplementary Table 4***). Notably, these 37 genes showed strong correlations with each other (***Fig. 2B***); we designated this cluster as the "GeneCards GC-Mongolian Hypoxia" (GGC-MH) gene set.

Similarly, intersection analysis using the top percentile subsets (100%, 75% and 25%) of the GeneCards list also showed overlaps, with nearly 50% of the top 25% genes overlapping with the Mongolian hypoxia-related genes (***Supplementary Fig. 2A*** and ***2B*** and ***Supplementary Table 4***). Subsequent GO functional enrichment analysis of the GGC-MH genes revealed significant enrichment in the "response to drug" category. This suggests that the specific activation of the hypoxia pathway in Mongolian GC patients may be intricately linked to chemotherapy response (***Fig. 2C***). Nevertheless, a more comprehensive understanding of how these GGC-MH genes impact the survival status of patients is warranted.

To address this, we conducted Kaplan–Meier survival analysis using the TCGA-STAD cohort. The results indicated that GC patients with high expression of GGC-MH genes, including *PGF*, *IGFBP1*, *AKAP12*, *ERRFI1*, *CAV1*, *ACKR3*, *SLC2A3*, and *ANGPTL4*, exhibited significantly poorer prognosis (***Fig. 2D***). Collectively, our findings suggest that tumors exhibiting pronounced hypoxic characteristics in Mongolian GC patients may possess enhanced invasiveness, consequently leading to an unfavorable clinical prognosis.

Multidrug resistance within the hypoxia-induced acidic tumor microenvironment

Hypoxia holds substantial clinical relevance in the context of cancer treatment. Hypoxic conditions within tumors can lead to a reduction in pH, resulting in an acidic tumor microenvironment (TME)[29]. Under

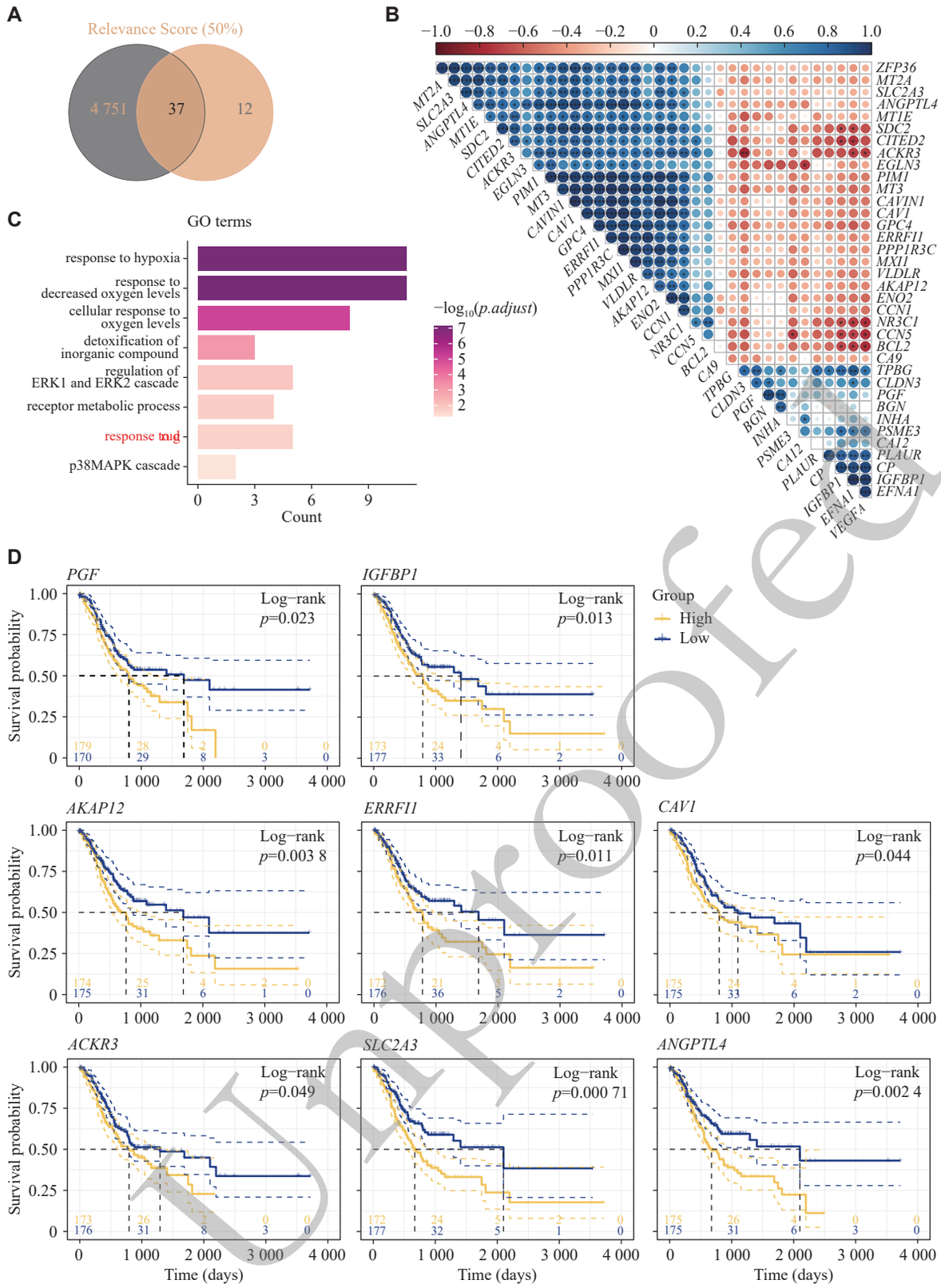

Fig. 2 **Prognostic analysis of hypoxia-related genes in Mongolian gastric cancer (GC).** A: Venn diagram depicting the specific and shared gene counts between Genecards-derived GC-related genes and Mongolian hypoxia-related genes. B: Correlation matrix of the Genecards-derived GC-Mongolian Hypoxia (GGC-MH) genes. The depth of the circle color indicates the strength of the correlation, while the size of the circle represents the absolute value of the correlation coefficient. $^{*}P < 0.05$, $^{**}P < 0.01$, and $^{***}P < 0.001$ by Pearson correlation test. C: Gene Ontology (GO) functional enrichment analysis of the GGC-MH genes. D: Kaplan–Meier survival curves evaluating the prognostic impact of *PGF*, *IGFBP1*, *AKAP12*, *ERRFI1*, *CAV1*, *ACKR3*, *SLC2A3*, and *ANGPTL4* in The Cancer Genome Atlas -Stomach Adenocarcinoma (TCGA-STAD) cohort (high expression *vs*. low expression, threshold: median expression).

hypoxia, cells rely primarily on glycolysis for ATP production due to the impaired efficiency of oxidative phosphorylation. In this pathway, glucose is metabolized into lactate. However, the insufficient oxidation of lactate under hypoxic conditions leads to its intracellular and extracellular accumulation, thereby driving the development of an acidic microenvironment[30-32]. Thus, we comprehensively examined alterations in genes encoding metabolic enzymes in Mongolian GC tumor tissues compared with adjacent non-tumor tissues. This analysis encompassed pathways related to glucose, lipid, and fatty acid metabolism (nine KEGG pathways, 471 genes) (***Supplementary Table 5***). Remarkable changes were noted in the expression of genes linked to glycolysis/gluconeogenesis and arachidonic acid metabolism among Mongolian GC patients (***Fig. 3A*** and ***Supplementary Fig. 3A***).

Given the complexity of metabolic processes and the limitations of the transcriptomic data at our disposal, we focused specifically on enzymes catalyzing the interconversion of pyruvate and lactate. Although multiple factors regulate this network, our data indicated that lactate dehydrogenase A (*LDHA*), which catalyzes the reduction of pyruvate to lactate, showed no significant change at the mRNA level. Conversely, lactate dehydrogenase B (*LDHB*), which participates in the oxidation of lactate to pyruvate,

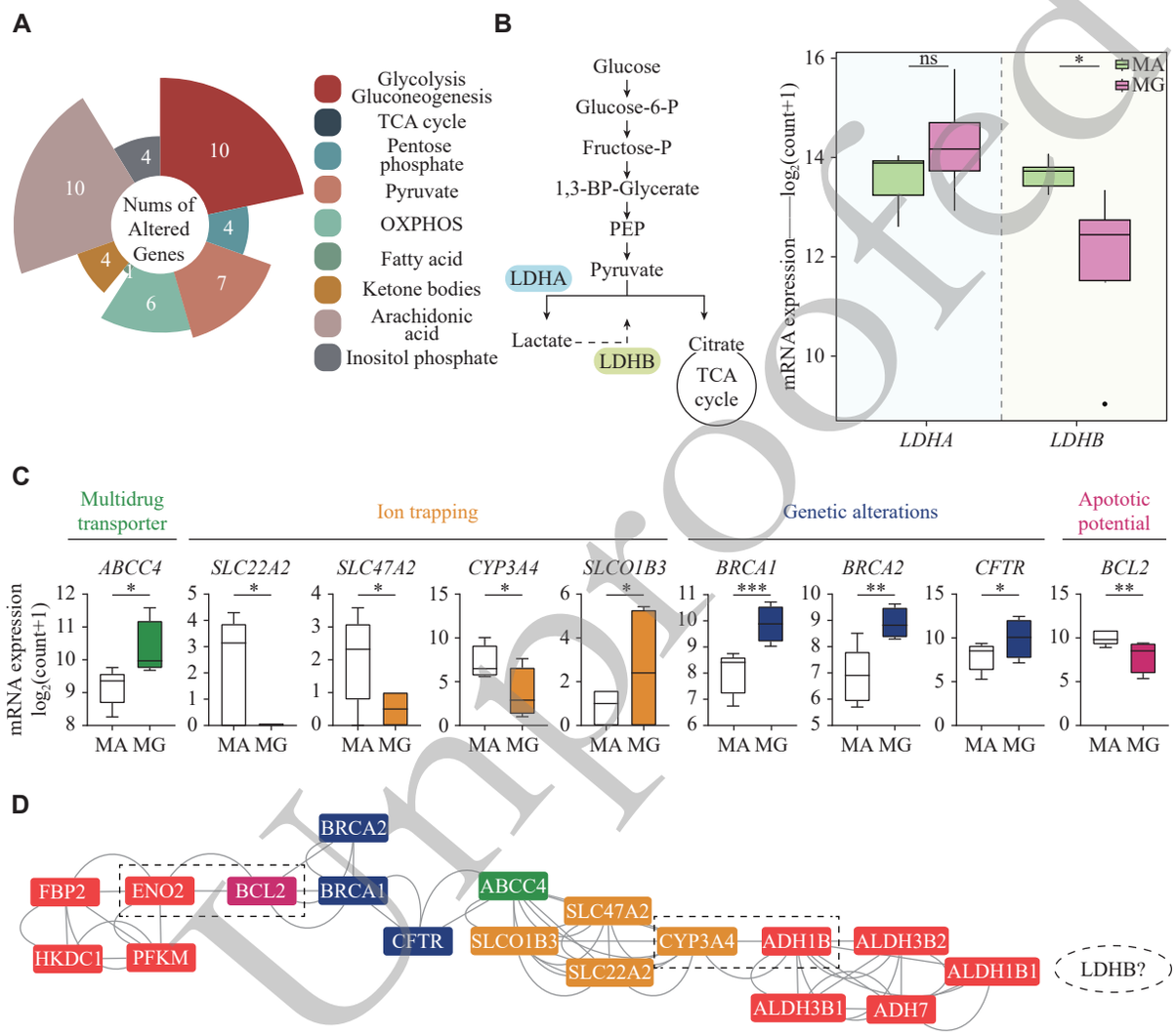

Fig. 3 **Association between hypoxic microenvironment and multidrug resistance in Mongolian gastric cancer (GC).** A: Nightingale rose diagram shows the numbers of altered genes across nine Kyoto Encyclopedia of Genes and Genomes (KEGG) metabolic pathways. B: Left: Glycolysis metabolic landscape. Right: RNA-seq expression levels of *LDHA* and *LDHB* in Mongolian GC tumor tissues (n = 4) compared with adjacent non-tumor tissues (n = 5). $^{*}P < 0.05$ by the Wald test in DESeq2. C: RNA-seq expression levels of *ABCC4*, *SLC22A2*, *SLC47A2*, *CYP3A4*, *SLCO1B3*, *BRCA1*, *BRCA2*, *CFTR* and *BCL2* in Mongolian GC tumor tissues (n = 4) compared with adjacent non-tumor tissues (n = 5). $^{*}P < 0.05$, $^{**}P < 0.01$, and $^{***}P < 0.001$ by the Wald test in DESeq2. D: Protein-protein interaction (PPI) network depicting functional associations between glycolysis-related differentially expressed genes and multidrug resistance. Abbreviation: MG, Mongolian GC tumor tissue; MA, Mongolian adjacent non-tumor tissue; ns: no significant.

showed a downregulation trend (***Fig. 3B***). This imbalance likely promotes lactate accumulation within the cells by hindering its clearance, consistent with previous conclusions. Simultaneously, we utilized GSEA to confirm the upregulation of glycolysis pathways in Mongolian GC tumor tissues (***Supplementary Fig. 3B***).

The aforementioned acidic TME is known to foster mechanisms contributing to multidrug resistance (MDR), including increased drug efflux transporter activity, reduced drug accumulation due to "ion trapping", genetic alterations, and diminished cellular apoptotic potential[29]. Among the genes associated with these four processes, the following exhibited altered expression in Mongolian GC tumors: *ABCC4* (in multidrug transporter), *SLC22A2*, *SLC47A2*, *CYP3A4*, *SLCO1B3* (in ion trapping), *BRCA1*, *BRCA2*, *CFTR* (in genetic alterations), and *BCL2* (in apoptotic potential) (***Fig. 3C*** **and** ***Supplementary Table 6***). Subsequently, we constructed a PPI network using these nine genes alongside glycolysis-related DEGs[33]. Network analysis revealed direct and indirect functional associations between glycolytic pathways and MDR mechanisms (***Fig. 3D***). Notably. LDHB was excluded from the network due to limited documented interactions in current databases. This absence highlights a gap in current knowledge, suggesting that further research on LDHB could provide valuable insights into its role within the hypoxia-induced acidic TME.

Hypoxia-induced alterations in cellular pharmacokinetics in Mongolian patients

The Mongolian population, traditionally characterized by a nomadic lifestyle, relies predominantly on a diet rich in meat and dairy products. Prolonged consumption of such high-protein and high-fat diets is implicated in the potential development of chronic gastritis and increased gastric acid secretion, thereby elevating the risk of GC[34-36]. Furthermore, cultural tendencies toward heavy alcohol consumption during festivals or special occasions and holidays may exacerbate gastric mucosal damage and chronic inflammation, further heightening GC susceptibility in this population.

To elucidate the distinctive mechanisms of GC driven by these specific lifestyles and dietary factors, we selected Han Chinese individuals residing in Inner Mongolia as a control group. PCA results indicated that the GC tumor tissues from Mongolian and Han patients did not exhibit complete separation (***Fig. 4A***). However, volcano plots and heatmaps revealed significant differences in gene expression profiles between the two groups, yielding 922 DEGs (***Fig. 4B*** **and** ***4C***). The most notable changes were observed in *PI3* and *KRT6B*. *PI3* encodes an elastase-specific inhibitor and plays a significant role during the course of hepatocellular carcinoma metastasis[37]. However, similar to KRT6B, the specific role of PI3 in GC remains poorly characterized, with limited literature dedicated to its function in this malignancy. KEGG and GO enrichment analyses indicated that the distinctions between Mongolian and Han patients were associated with drug metabolism processes, particularly those involving cytochrome P450 (CYP450) enzymes (***Fig. 4D*** and ***4E***). In contrast, analyses of tumor and adjacent non-tumor tissues from Han GC patients revealed no significant activation of the hypoxia pathway (***Supplementary Fig. 4A-4D***). Consistently, validation using an independent cohort[38] further confirmed that the hypoxia pathway was not activated in GC tissues of the Han population (***Supplementary Fig. 4E***).

Given the established regulatory effect of hypoxia on CYP450, we hypothesized that variations in hypoxia lead to changes in CYP450 in Mongolian GC patients. Using a strategy similar to that for identifying Mongolian hypoxia-related genes from MSigDB, we curated a total of 142 Mongolian CYP450-related genes (***Supplementary Table 7***). Through the construction of a PPI network to analyze the interaction between hypoxia-related genes and CYP450-related genes in Mongolian GC patients, we identified the CYP450 gene directly affected by hypoxia (***Supplementary Fig. 4F***).

Pharmacokinetics encompasses the absorption, distribution, metabolism, and excretion (ADME) of drugs, with metabolism playing a pivotal role[39]. CYP450 enzyme activity directly determines drug metabolic rates, significantly influencing systemic drug concentration and duration. Variations in the expression levels and activity of CYP450 enzymes among individuals contribute to the observed individual differences in drug metabolism dynamics[40, 41]. Furthermore, as previously mentioned, both multidrug transporters and ion trapping mechanisms collectively influence drug distribution and metabolism[29]. Therefore, we focused on the ADME process in Mongolian GC patients. We first extracted a list of 298 ADME-related genes from the pharmaADME consortium (www.pharmaadme.org), encompassing phase I and phase II drug-metabolizing enzymes, transport proteins, and modifiers. We then identified ADME-related genes exhibiting significant differential expression between tumor and adjacent non-tumor tissues, in both Mongolian and Han cohorts separately

(***Fig. 4F*** and ***Supplementary Fig. 4G***). Compared with the Han population, 28 genes showed Mongolian-specific alterations in tumor tissues. Among them, phase I drug-metabolizing enzymes and transporters accounted for the vast majority (***Fig. 4G***).

Superior cellular pharmacokinetics of paclitaxel, oxaliplatin and tegafur–gimeracil–oteracil potassium capsules (TGO) in Mongolian GC cells

Based on our comprehensive genomic analysis of Mongolian GC, we investigated ethnic differences in chemotherapy responses. According to the "Guidelines for the Diagnosis and Treatment of Gastric Cancer" published by the National Health Commission of China (2022 edition), commonly used systemic chemotherapy drugs include fluorouracil, capecitabine, TGO, cisplatin, oxaliplatin, paclitaxel, docetaxel, irinotecan, and epirubicin. To elucidate the metabolic and transport characteristics of these drugs, we consulted the Drugbank database[42] and found that their metabolism in the body primarily relies on specific metabolic enzymes and transporters (***Supplementary Fig. 5A***). Further analysis indicated that, in both Mongolian and Han GC patients, alterations in drug transporter expression were more pronounced than those in metabolic enzymes (***Fig. 5A***).

Drug sensitivity analysis offers comprehensive insights into patient responses to diverse medications[43]. Using the oncoPredict algorithm, we conducted drug sensitivity analysis on GC tumor tissues from both Mongolian and Han populations for nine chemotherapy drugs, obtaining valid predictions for seven. Based on predicted IC_{50} values, these chemotherapy drugs were stratified into three categories: relatively sensitive (paclitaxel, docetaxel, and epirubicin), less sensitive (fluorouracil, cisplatin, oxaliplatin, and irinotecan), and two additional drugs (capecitabine and TGO), which were analyzed separately (***Fig. 5B*** and ***5C***). To experimentally validate these computational predictions, we assessed

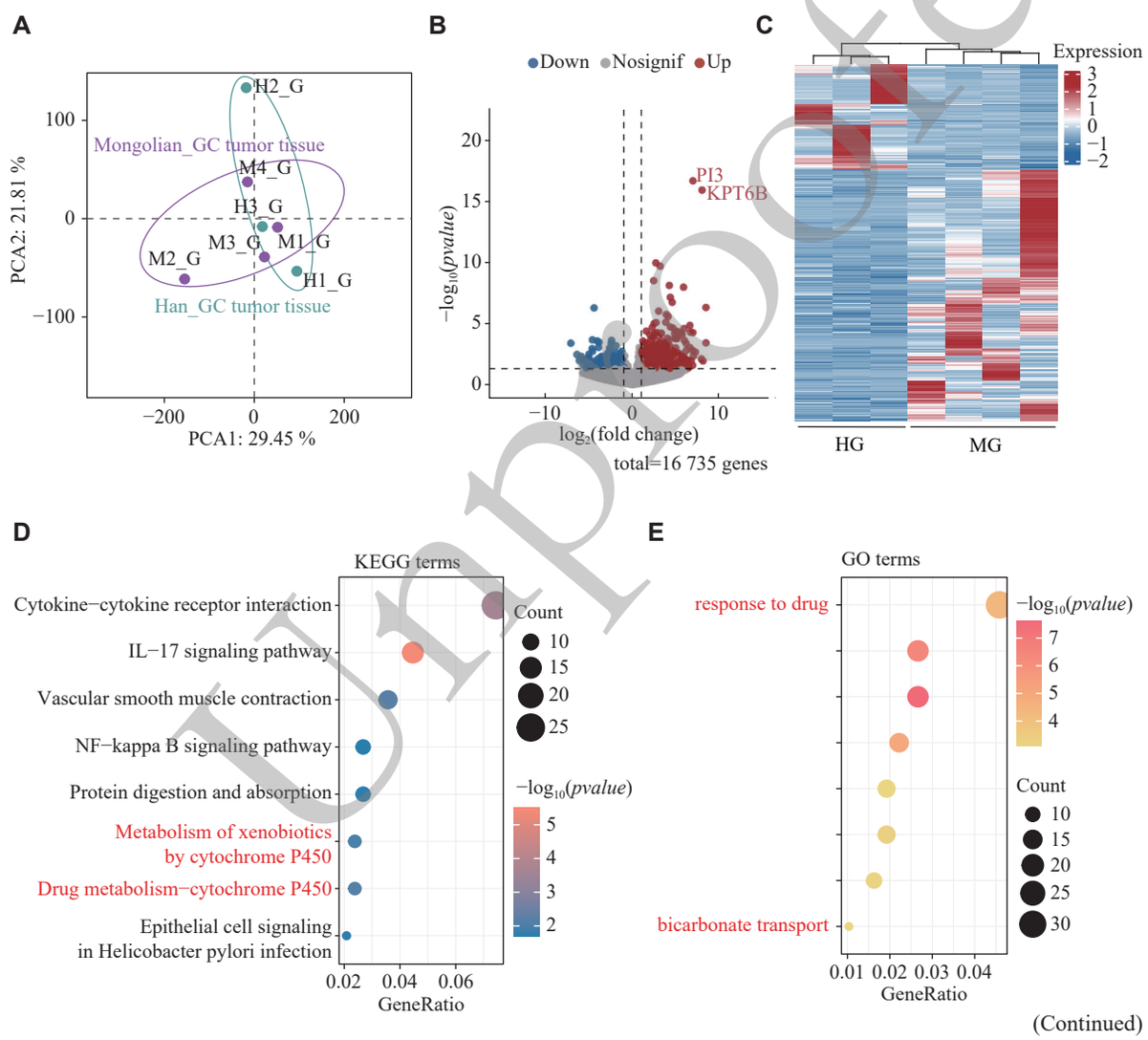

(Continued)

(Continued)

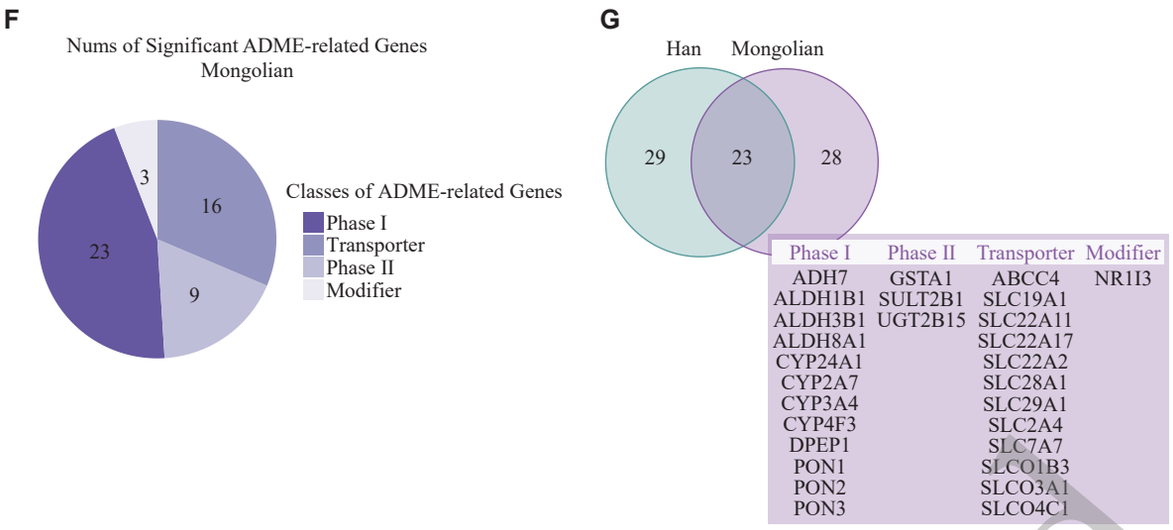

Fig. 4 **Comparative transcriptomic analysis of gastric cancer (GC) between Mongolian and Han Chinese populations.** A: PCA illustrates the distribution of samples along principal components (Mongolian GC tumor tissues *vs*. Han GC tumor tissues). Each point represents an individual sample (Han Tumor tissues: n = 3; Mongolian Tumor tissues: n = 4). B: Volcano plot visualizing differentially expressed genes (DEGs) by Wald test in DESeq2. Red dots represent upregulated genes ($^*P < 0.05$; fold change > 2), blue dots represent downregulated genes ($^*P < 0.05$; fold change < −2), and gray dots represent genes with no significant differential expression, Wald test in DESeq2. C: Heatmap of DEGs is shown (Han Tumor tissues: n = 3; Mongolian Tumor tissues: n = 4). D and E: KEGG pathway enrichment analysis (D) and GO functional enrichment analysis (E) of pathways enriched in Mongolian GC tumor tissues compared with Han GC tumor tissues. F: Pie plot shows the numbers of significant ADME-related genes in Mongolian. G: Venn diagram depicting the specific and shared ADME-related genes counts between Mongolian and Han Chinese GC tumor tissues. Abbreviations: ADME, absorption, distribution, metabolism, and excretion; GO, Gene Ontology; KEGG: Kyoto Encyclopedia of Genes and Genomes; PCA: principal component analysis; HG, Han GC tumor tissue; MG, Mongolian GC tumor tissue.

the response of the SGC-7 901 human GC cell line to paclitaxel and oxaliplatin. Consistent with the oncoPredict predictions, SGC-7901 cells exhibited relatively higher sensitivity to paclitaxel (IC_{50} = 7.09 nmol/L) and markedly lower sensitivity to oxaliplatin (IC_{50} = 7.13 μmol/L) (***Supplementary Fig. 5B*** and ***5C***).

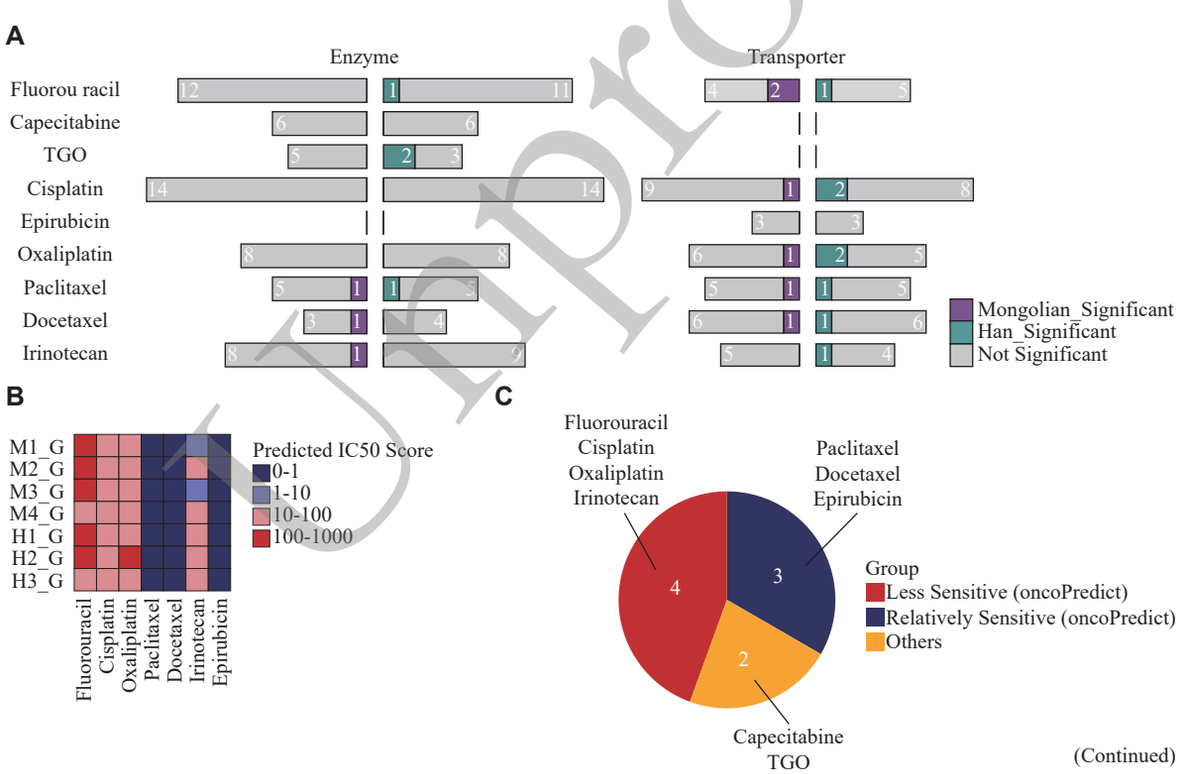

(Continued)

(Continued)

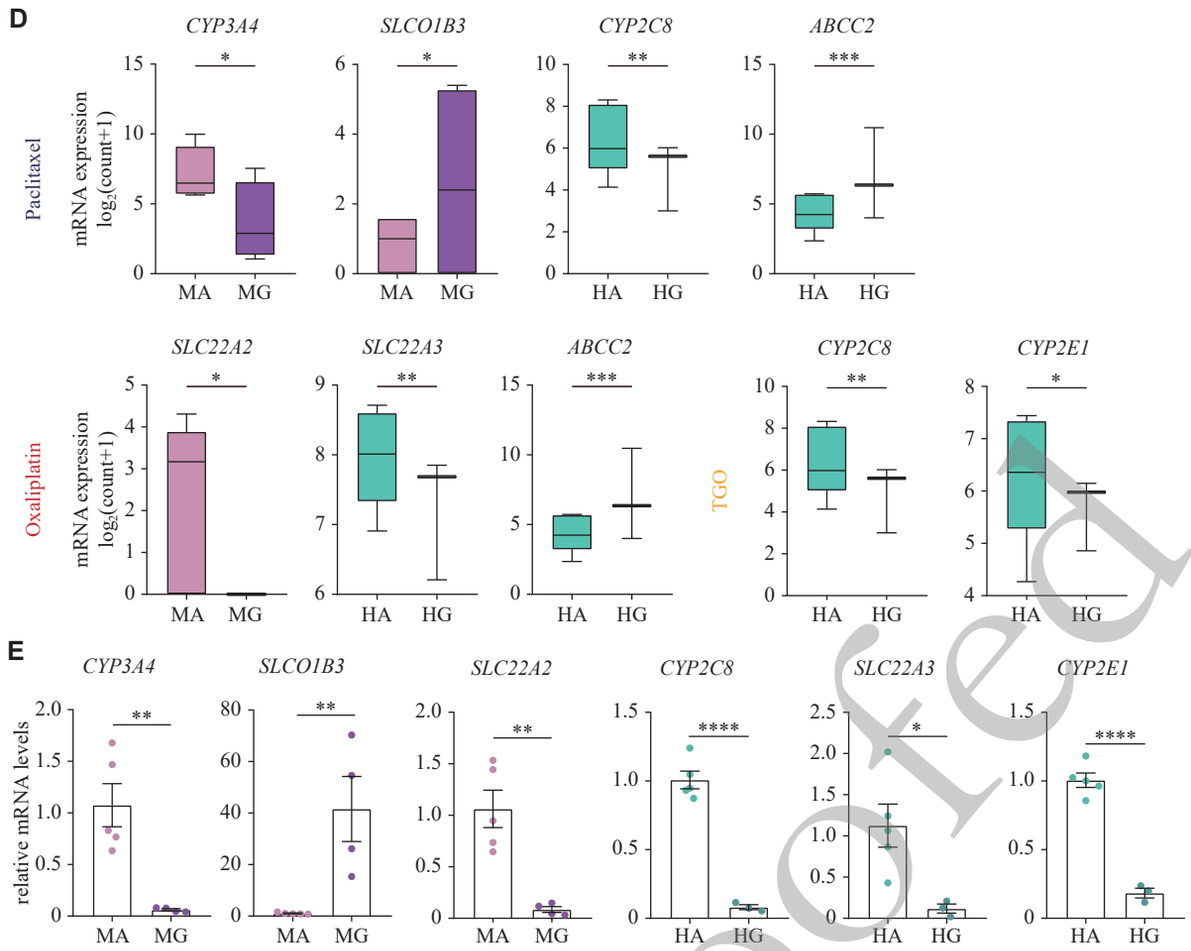

Fig. 5 **Chemotherapy drugs sensitivity analysis in Mongolian and Han Chinese gastric cancer (GC) patients.** A: Numbers of significant enzymes and transporters for GC chemotherapy drugs in Mongolian and Han populations. B: Heatmap of predicted IC_{50} score for chemotherapy drugs in Mongolian and Han GC tumor tissues. C: Pie plot shows the numbers of relatively sensitive drugs, less sensitive drugs predicted by OncoPredict, and remaining drugs. D: RNA-seq expression levels of *CYP3A4*, *SLCO1B3* and *SLC22A2* in Mongolian GC tumor tissues (n = 4) versus adjacent non-tumor tissues (n = 5), *CYP2C8*, *ABCC2*, *SLC22A3* and *CYP2E1* in Han GC tumor tissues (n = 3) and versus adjacent non-tumor tissues (n = 5). $^{*}P < 0.05$, $^{**}P < 0.01$, and $^{***}P < 0.001$ by the Wald test in DESeq2. E: Relative mRNA expression levels of *CYP3A4*, *SLCO1B3*, and *SLC22A2* in Mongolian GC tumor tissues (n = 4) and adjacent non-tumor tissues (n = 5), and *CYP2C8*, *SLC22A3*, and *CYP2E1* in Han GC tumor tissues (n = 3) and adjacent non-tumor tissues (n = 5). Data were normalized to the paired adjacent non-tumor tissues for each sample and are presented as mean ± standard error of the mean (SEM). $^{*}P < 0.05$, $^{**}P < 0.01$, $^{***}P < 0.001$ and $^{****}P < 0.000\,1$ by two-tailed Student's t-test. Abbreviations: IC_{50}, half-maximal inhibitory concentration; ns: no significant; TGO, tegafur–gimeracil–oteracil potassium capsules; HG, Han GC tumor tissue; HA, Han adjacent non-tumor tissue; MG, Mongolian GC tumor tissue; MA, Mongolian adjacent non-tumor tissue.

For relatively sensitive chemotherapy drugs, our observations revealed superior cellular pharmacokinetic characteristics for paclitaxel in Mongolian GC patients. Despite reduced RNA expression levels of metabolic enzymes *CYP3A4* (in Mongolian) and *CYP2C8* (in Han), the advantageous expression of the absorption transporter *SLCO1B3* in Mongolian patients facilitated drug absorption; however, elevated expression of the efflux transporter *ABCC2* may contribute to diminished drug retention in tumor cells among Han patients. Concerning the less sensitive chemotherapy drug oxaliplatin, expression of ethnicity-specific absorption transporters *SLCC22A2* (in Mongolian patients) and *SLCC22A3* (in Han patients) was downregulated in both groups, while upregulation of the efflux transporter *ABCC2* in Han patients further impeded drug accumulation. Finally, for one of the remaining chemotherapy drugs, TGO exhibited pharmacokinetic features favorable for Mongolian patients, with only the expression of Han ethnicity-specific metabolic enzymes *CYP2C8* and *CYP2E1* being downregulated (***Fig. 5D***). These transcriptional changes were also confirmed by RT-qPCR (***Fig. 5E***).

To further validate these findings in a clinical context, we incorporated progression-free survival

(PFS) data from GC patients treated at Chifeng Municipal Hospital. After applying predefined inclusion and exclusion criteria, 45 Han and 31 Mongolian patients were eligible for analysis. To ensure treatment comparability, we restricted the analysis to male patients receiving the same chemotherapy regimen (oxaliplatin + TGO), including 20 Han patients and 14 Mongolian patients. The results

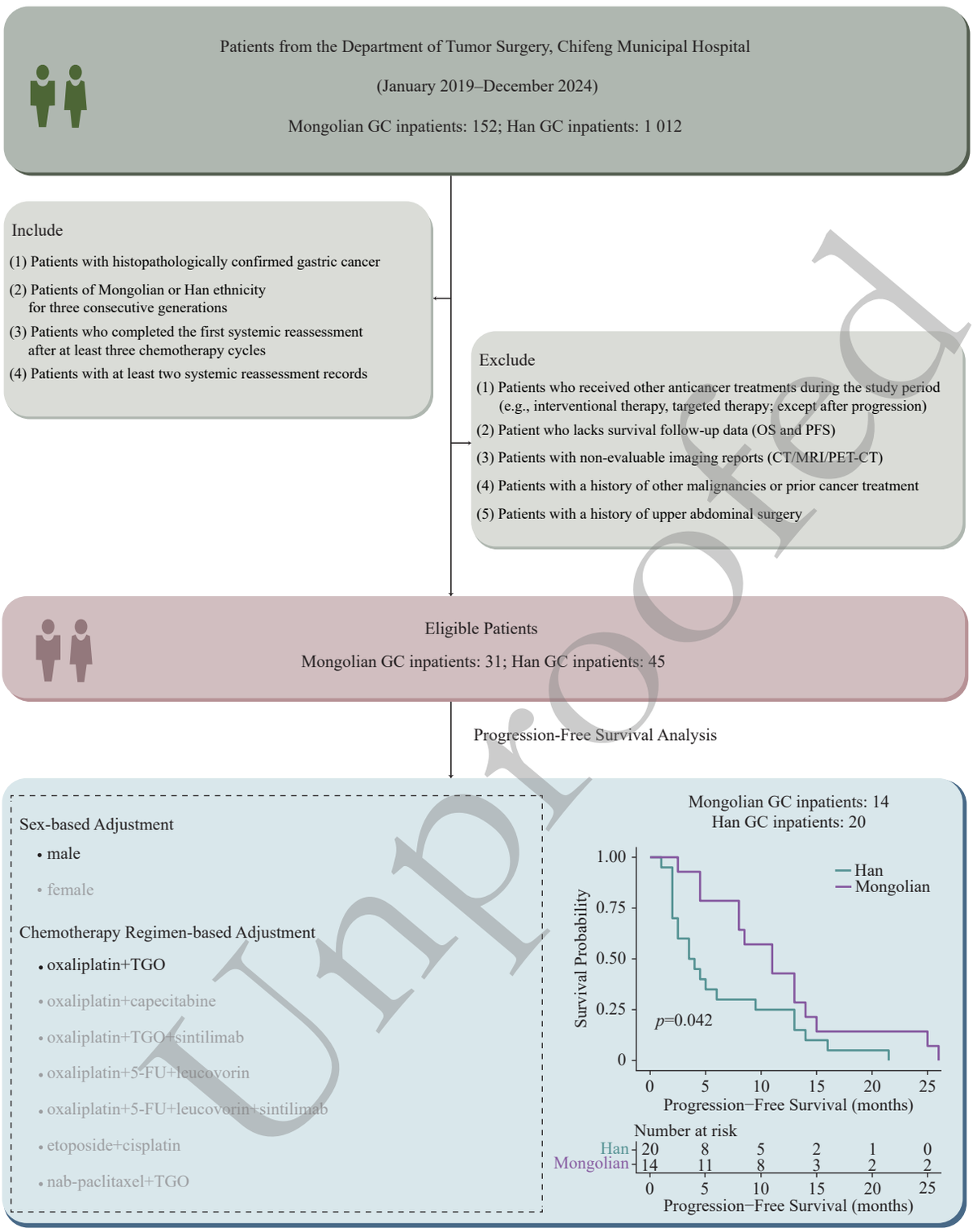

Fig. 6 **Clinical cohort response data and progression-free survival (PFS) comparison between Mongolian and Han gastric cancer (GC) patients.** PFS survival analysis was performed by Log-rank test. Abbreviations: TGO, tegafur–gimeracil–oteracil potassium capsules; 5-FU, 5-Fluorouracil; OS, overall survival; CT, computed tomography; MRI, magnetic resonance imaging; PET-CT, positron emission tomography-computed tomography.

showed that Mongolian patients exhibited prolonged PFS compared with Han patients, providing real-world evidence supporting the cellular pharmacokinetic patterns predicted in our model (***Fig. 6***). Overall, by integrating transporter (SLC and ABC families) and metabolic enzyme (CYP family) expression profiles, we identified distinct cellular pharmacokinetic advantages for paclitaxel, oxaliplatin, and TGO in Mongolian GC cells, offering mechanistic insights into ethnicity-related differences in chemotherapeutic response.

Discussion

In recent years, the incidence and mortality rates of GC have risen notably in Asian countries[44], followed by South America and parts of Central Asia, whereas Europe and North America exhibit comparatively lower rates[45-47]. Against this backdrop, significant incongruity exists in research findings regarding postoperative adjuvant chemotherapy across different regions. Consequently, it is critical to examine whether current GC chemotherapy regimens exhibit unexpected therapeutic efficacy in Mongolian patients. The "All of Us" project aims to enhance the diversity of biological research by investigating the genetics of individuals from underrepresented racial and ethnic minorities in the USA, thereby facilitating accurate diagnosis and treatment of diseases for individuals from diverse backgrounds[48]. Inspired by this model, our study compares the transcriptional characteristics of Mongolian GC patients with those of the Han population in China. Our primary objective is to improve the understanding of the molecular mechanisms underlying these ethnic disparities to advance precise treatment for Mongolian GC patients.

Within China's diverse ethnic landscape, the Han and the Mongolian populations display discernible differences shaped by a complex interplay of genetic, environmental, lifestyle, and cultural factors. Notably, genetic variations play a pivotal role in elucidating variations in cancer manifestation among diverse individuals or populations[49, 50]. These disparities encompass differences in somatic mutation profiles, germline variants, and gene expression levels, which ultimately influence individual cancer susceptibility and tumor biological behavior[51]. While recent research has presented evidence highlighting disparities between Mongoliansand Han Chinese in specific malignancies such as pancreatic and lung cancers[52, 53], data regarding GC in this context remain notably scarce.

This study introduces, for the first time, the specific activation of the hypoxia pathway in GC within the Mongolian population. Comparative analysis with Han Chinese GC patients revealed disparities in drug metabolism, particularly involving CYP450 enzymes. While traditional pharmacokinetics aims to explore the macroscopic processes of drug absorption, distribution, metabolism, and excretion in the body, cellular pharmacokinetics examines these dynamics at the microscopic cellular level[54, 55]. In this study, we concentrated solely on the ADME-related gene expression profiles within GC cells. By analyzing ethnic-specific alterations in these genes in Mongolian and Han cohorts, we identified three chemotherapy drugs that exhibit more efficient cellular pharmacokinetics specifically in Mongolian GC cells (***Fig. 7***). Furthermore, certain potential targets identified in the Mongolian population, such as *KRT6B*, *PI3*, *CYP3A4*, *SLCO1B3*, and *SLC22A2*, necessitate further investigation in larger-scale studies. Additionally, the role of *LDHB* in oncogenesis warrants in-depth exploration across various cancer types, extending beyond GC.

We acknowledge some limitations of the current work, which present opportunities for future developments. First, the modest sample size may have yielded insufficient statistical power; we therefore applied more stringent criteria for defining DEGs. Second, the absence of additional Mongolian GC datasets precluded external validation, and owing to regional disparities in socioeconomic development—multicenter recruitment remains challenging; we therefore corroborated the key findings experimentally. Finally, the precise molecular mechanisms by which the acidic tumor microenvironment modulates enzymes and transporters remain undefined, underscoring the need for deeper mechanistic investigations. Nonetheless, our work identifies potential therapeutic targets and expands the range of options for the treatment of GC. These findings have the potential to enhance treatment efficacy while minimizing unnecessary drug side effects. In summary, we enriched the comprehension of GC etiology through a transcriptomic lens andadvocated for the customization of chemotherapeutic interventions for the Mongolian population.

Funding

This study was jointly supported by the Natural

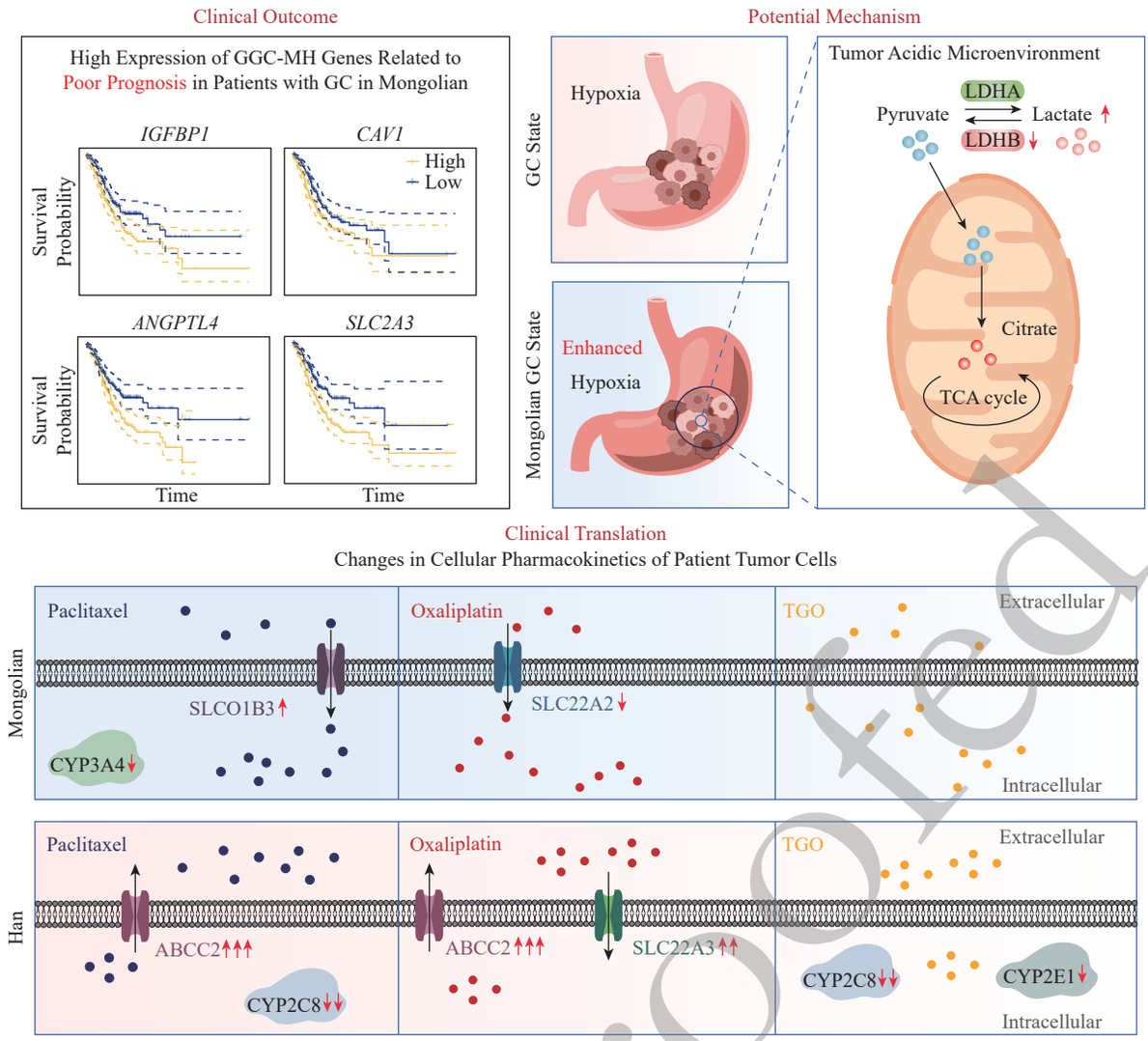

Fig. 7 **Workflow of the research.**

Science Research Project of Chifeng, Inner Mongolia Autonomous Region (Grant No. SZR21174 to X.W.) and the Jiangsu Funding Program for Excellent Postdoctoral Talent (Grant NO. 2022ZB431 to Y.Z.).

Acknowledgements

We are grateful to Dr. Jia-Li Wang (Department of Hematology and Oncology, Children's Hospital of Nanjing Medical University) for her expert guidance on cellular pharmacokinetics analysis and cancer chemotherapy.

Additional information

The online version contains supplementary material available at http://www.jbr-pub.org.cn/article/doi/10.7555/JBR.39.20250238?pageType=en. The data that support the findings of this study and all code used in this study are available from the corresponding author upon reasonable request.

References

[1] O'Donnell PH, Dolan ME. Cancer pharmacoethnicity: ethnic differences in susceptibility to the effects of chemotherapy[J]. *Clin Cancer Res*, 2009, 15(15): 4806–4814.

[2] Brahmer J, Reckamp KL, Baas P, et al. Nivolumab versus docetaxel in advanced squamous-cell non-small-cell lung cancer[J]. *N Engl J Med*, 2015, 373(2): 123–135.

[3] Bianchi DW, Brennan PF, Chiang MF, et al. The All of US Research Program is an opportunity to enhance the diversity of US biomedical research[J]. *Nat Med*, 2024, 30(2): 330–333.

[4] The All of Us Research Program Genomics Investigators. Genomic data in the All of Us Research Program[J]. *Nature*, 2024, 627(8003): 340–346.

[5] Bai H, Guo X, Narisu N, et al. Whole-genome sequencing of

175 Mongolians uncovers population-specific genetic architecture and gene flow throughout North and East Asia[J]. *Nat Genet*, 2018, 50(12): 1696–1704.

[6] Wang F, Zhang X, Tang L, et al. The Chinese Society of Clinical Oncology (CSCO): clinical guidelines for the diagnosis and treatment of gastric cancer, 2023[J]. *Cancer Commun (Lond)*, 2024, 44(1): 127–172.

[7] Ajani JA, D'Amico TA, Bentrem DJ, et al. Gastric cancer, version 2.2022, NCCN clinical practice guidelines in oncology[J]. *J Natl Compr Canc Netw*, 2022, 20(2): 167–192.

[8] Gantuya B, Oyuntsetseg K, Bolor D, et al. Evaluation of serum markers for gastric cancer and its precursor diseases among high incidence and mortality rate of gastric cancer area[J]. *Gastric Cancer*, 2019, 22(1): 104–112.

[9] Jin G, Lv J, Yang M, et al. Genetic risk, incident gastric cancer, and healthy lifestyle: a meta-analysis of genome-wide association studies and prospective cohort study[J]. *Lancet Oncol*, 2020, 21(10): 1378–1386.

[10] Livak KJ, Schmittgen TD. Analysis of relative gene expression data using real-time quantitative PCR and the $2^{-\Delta\Delta C_T}$ method[J]. *Methods*, 2001, 25(4): 402–408.

[11] Ringnér M. What is principal component analysis?[J]. *Nat Biotechnol*, 2008, 26(3): 303–304.

[12] Ito K, Murphy D. Application of *ggplot2* to Pharmacometric Graphics[J]. *CPT Pharmacometrics Syst Pharmacol*, 2013, 2(10): e79.

[13] Love MI, Huber W, Anders S. Moderated estimation of fold change and dispersion for RNA-seq data with DESeq2[J]. *Genome Biol*, 2014, 15(12): 550.

[14] Ashburner M, Ball CA, Blake JA, et al. Gene ontology: tool for the unification of biology[J]. *Nat Genet*, 2000, 25(1): 25–29.

[15] Yu G, Wang L, Han Y, et al. clusterProfiler: an R package for comparing biological themes among gene clusters[J]. *Omics*, 2012, 16(5): 284–287.

[16] Kanehisa M, Goto S. KEGG: kyoto encyclopedia of genes and genomes[J]. *Nucleic Acids Res*, 2000, 28(1): 27–30.

[17] Schubert M, Klinger B, Klünemann M, et al. Perturbation-response genes reveal signaling footprints in cancer gene expression[J]. *Nat Commun*, 2018, 9(1): 20.

[18] Subramanian A, Tamayo P, Mootha VK, et al. Gene set enrichment analysis: a knowledge-based approach for interpreting genome-wide expression profiles[J]. *Proc Natl Acad Sci U S A*, 2005, 102(43): 15545–15550.

[19] Maeser D, Gruener RF, Huang RS. oncoPredict: an R package for predicting *in vivo* or cancer patient drug response and biomarkers from cell line screening data[J]. *Brief Bioinform*, 2021, 22(6): bbab260.

[20] Song Q, Yu H, Cheng Y, et al. Bladder cancer-derived exosomal KRT6B promotes invasion and metastasis by inducing EMT and regulating the immune microenvironment[J]. *J Transl Med*, 2022, 20(1): 308.

[21] López-Sánchez LM, Jurado-Gámez B, Feu-Collado N, et al. Exhaled breath condensate biomarkers for the early diagnosis of lung cancer using proteomics[J]. *Am J Physiol Lung Cell Mol Physiol*, 2017, 313(4): L664–L676.

[22] Janjigian YY, Kawazoe A, Yañez P, et al. The KEYNOTE-811 trial of dual PD-1 and HER2 blockade in HER2-positive gastric cancer[J]. *Nature*, 2021, 600(7890): 727–730.

[23] Katoh Y, Katoh M. Comparative integromics on FAT1, FAT2, FAT3 and FAT4[J]. *Int J Mol Med*, 2006, 18(3): 523–528.

[24] Waldum HL, Hauso Ø, Fossmark R. The regulation of gastric acid secretion–clinical perspectives[J]. *Acta Physiol (Oxf)*, 2014, 210(2): 239–256.

[25] Li S, Cong X, Gao H, et al. Tumor-associated neutrophils induce EMT by IL-17a to promote migration and invasion in gastric cancer cells[J]. *J Exp Clin Cancer Res*, 2019, 38(1): 6.

[26] The Cancer Genome Atlas Research Network, Weinstein JN, Collisson EA, et al. The Cancer Genome Atlas Pan-Cancer analysis project[J]. *Nat Genet*, 2013, 45(10): 1113–1120.

[27] Chen S, Fang X, Wang Q, et al. PHD/HIF-1 upregulates CA12 to protect against degenerative disc disease: a human sample, *in vitro* and *ex vivo* study[J]. *Lab Invest*, 2016, 96(5): 561–569.

[28] Waheed A, Sly WS. Carbonic anhydrase XII functions in health and disease[J]. *Gene*, 2017, 623: 33–40.

[29] Jing X, Yang F, Shao C, et al. Role of hypoxia in cancer therapy by regulating the tumor microenvironment[J]. *Mol Cancer*, 2019, 18(1): 157.

[30] Lunt SY, Vander Heiden MG. Aerobic glycolysis: meeting the metabolic requirements of cell proliferation[J]. *Annu Rev Cell Dev Biol*, 2011, 27: 441–464.

[31] Zhao R, Jiang S, Zhang L, et al. Mitochondrial electron transport chain, ROS generation and uncoupling (Review)[J]. *Int J Mol Med*, 2019, 44(1): 3–15.

[32] Vander Heiden MG, Cantley LC, Thompson CB. Understanding the Warburg effect: the metabolic requirements of cell proliferation[J]. *Science*, 2009, 324(5930): 1029–1033.

[33] Szklarczyk D, Kirsch R, Koutrouli M, et al. The STRING database in 2023: protein-protein association networks and functional enrichment analyses for any sequenced genome of interest[J]. *Nucleic Acids Res*, 2023, 51(D1): D638–D646.

[34] Yang P, Zhou Y, Chen B, et al. Overweight, obesity and gastric cancer risk: results from a meta-analysis of cohort studies[J]. *Eur J Cancer*, 2009, 45(16): 2867–2873.

[35] Zhang R, Li H, Li N, et al. Risk factors for gastric cancer: a large-scale, population-based case-control study[J]. *Chin Med J (Engl)*, 2021, 134(16): 1952–1958.

[36] Deng W, Jin L, Zhuo H, et al. Alcohol consumption and risk of stomach cancer: a meta-analysis[J]. *Chem Biol Interact*, 2021, 336: 109365.

[37] Wang C, Liao Y, He W, et al. Elafin promotes tumour metastasis and attenuates the anti-metastatic effects of erlotinib via binding to EGFR in hepatocellular carcinoma[J]. *J Exp Clin Cancer Res*, 2021, 40(1): 113.

[38] Li L, Zhu Z, Zhao Y, et al. FN1, SPARC, and SERPINE1 are highly expressed and significantly related to a poor prognosis

of gastric adenocarcinoma revealed by microarray and bioinformatics[J]. *Sci Rep*, 2019, 9(1): 7827.

[39] Fan J, de Lannoy IAM. Pharmacokinetics[J]. *Biochem Pharmacol*, 2014, 87(1): 93–120.

[40] Zanger UM, Schwab M. Cytochrome P450 enzymes in drug metabolism: regulation of gene expression, enzyme activities, and impact of genetic variation[J]. *Pharmacol Ther*, 2013, 138(1): 103–141.

[41] van Schaik RH. CYP450 pharmacogenetics for personalizing cancer therapy[J]. *Drug Resist Updat*, 2008, 11(3): 77–98.

[42] Wishart DS, Knox C, Guo AC, et al. DrugBank: a knowledgebase for drugs, drug actions and drug targets[J]. *Nucleic Acids Res*, 2008, 36(suppl_1): D901–D906.

[43] Costello JC, Heiser LM, Georgii E, et al. A community effort to assess and improve drug sensitivity prediction algorithms[J]. *Nat Biotechnol*, 2014, 32(12): 1202–1212.

[44] Sung H, Ferlay J, Siegel RL, et al. Global cancer statistics 2020: GLOBOCAN estimates of incidence and mortality worldwide for 36 cancers in 185 countries[J]. *CA Cancer J Clin*, 2021, 71(3): 209–249.

[45] Wong MCS, Huang J, Chan PSF, et al. Global incidence and mortality of gastric cancer, 1980–2018[J]. *JAMA Netw Open*, 2021, 4(7): e2118457.

[46] Morgan E, Arnold M, Camargo MC, et al. The current and future incidence and mortality of gastric cancer in 185 countries, 2020–40: a population-based modelling study[J]. *EClinicalMedicine*, 2022, 47: 101404.

[47] GBD 2017 Stomach Cancer Collaborators. The global, regional, and national burden of stomach cancer in 195 countries, 1990–2017: a systematic analysis for the Global Burden of Disease study 2017[J]. *Lancet Gastroenterol Hepatol*, 2020, 5(1): 42–54.

[48] Ginsburg GS, Denny JC, Schully SD. Data-driven science and diversity in the All of Us Research Program[J]. *Sci Transl Med*, 2023, 15(726): eade9214.

[49] Turajlic S, Sottoriva A, Graham T, et al. Resolving genetic heterogeneity in cancer[J]. *Nat Rev Genet*, 2019, 20(7): 404–416.

[50] Li B, Cai Y, Chen C, et al. Genetic variants that impact alternative polyadenylation in cancer represent candidate causal risk loci[J]. *Cancer Res*, 2023, 83(21): 3650–3666.

[51] Martínez-Jiménez F, Muiños F, Sentís I, et al. A compendium of mutational cancer driver genes[J]. *Nat Rev Cancer*, 2020, 20(10): 555–572.

[52] Xu J, Liao K, Fu Z, et al. Screening differentially expressed genes of pancreatic cancer between Mongolian and Han people using bioinformatics technology[J]. *BMC Cancer*, 2020, 20(1): 298.

[53] Zhang J, Liu X, Huang Z, et al. T cell-related prognostic risk model and tumor immune environment modulation in lung adenocarcinoma based on single-cell and bulk RNA sequencing[J]. *Comput Biol Med*, 2023, 152: 106460.

[54] Zhou F, Zhang J, Li P, et al. Toward a new age of cellular pharmacokinetics in drug discovery[J]. *Drug Metab Rev*, 2011, 43(3): 335–345.

[55] Zhang J, Zhou F, Lu M, et al. Pharmacokinetics-pharmacology disconnection of herbal medicines and its potential solutions with cellular pharmacokinetic-pharmacodynamic strategy[J]. *Curr Drug Metab*, 2012, 13(5): 558–576.